Impurity composition and cathodoluminescence of type IIb HPHT diamond with boron concentration up to 60 ppm

© V.A. Kravets[1], I.V. Klepikov[2,3], E.A. Vasilev[4]

[1] Ioffe Institute, St. Petersburg, Russia
[2] LLC „NPK „Almaz", 197706 St. Petersburg, Russia
[3] Laboratory „Diamond Microwave Electronics" RTU MIREA, 119454 Moscow, Russia
[4] St. Petersburg Mining University, St. Petersburg, Russia

e-mail: vladislav2033@yandex.ru

A single-crystal multi-sector plate of type IIb HPHT diamond was studied using local cathodoluminescence (CL) at a temperature of 77 K and IR spectroscopy. The features of the CL growth sectors (100), (110), (113), (111) of diamond grown using the HPHT technology were studied. In the luminescence of the band with a maximum of 2.3 eV in each of the growth sectors, two components with different decay times, located in the ranges of $2-11\,\mu$s and $19-96\,\mu$s, were detected. The decay time of the band with a maximum of 3.0 eV is less than 100 ns. It is shown that each growth face is a separate luminescent material with its own characteristic CL properties.

Keywords: HPHT diamond, cathodoluminescence, growth sector, internal structure, type IIb diamond.

Introduction

Type IIb diamond is a semiconductor with a band gap of 5.5 eV and an acceptor level of 0.37 eV of the boron atom that replaces carbon. As the boron concentration increases, an impurity band is formed with a lower boundary of about 0.12 eV [1]. Natural and synthetic diamonds contain in their structure many defect-impurity centers responsible for luminescence [2–5]. The luminescence of type IIb diamonds has been repeatedly studied, and its recombination nature is now recognized (recombination of electrons and holes on donor-acceptor (DA) pairs). The model of the luminescence center proposed in [2,6,7] discusses a nitrogen dimer as the donor and a substitutional boron atom as the acceptor. It is shown that the luminescent characteristics of the band should depend on the concentration of the doping impurity in diamonds (boron and nitrogen), however, systematic studies are complicated by the difficulty of controlling the defect-impurity composition. In addition, all types of diamonds, when excited by quanta with an energy of more than 5.5 eV, demonstrate a wide structureless „band A" in the region of 2.3–3.2 eV [2,6,7]. The nature of the „band A" luminescence has not been fully clarified to date. One version is that, this band is associated with intrinsic defects in the crystalline structure of diamond [8,9,10], in particular, with the sp^2 hybridization of electron orbitals on dislocations and stacking faults of carbon atoms [6 ,7]. This energy range is likely to have an overlap of bands of different origins.

Modern methods of diamond synthesis make it possible to control the presence and concentration of doping impurities in the process of growth. There are two main competing methods for growing diamonds: high-pressure high temperature (HPHT) method and chemical vapor-phase deposition (CVD). Previously, high boron concentrations were achieved in both CVD and HPHT diamonds. The CVD method, due to the layer-by-layer deposition of diamond, currently has some advantages in technical applications, but HPHT diamonds in certain growth sectors are a more homogeneous material with fewer internal stresses.

In this study, data was obtained on the spectral-time characteristics of luminescence in different growth sectors of a type IIb diamond single crystal with a boron concentration of up to 60 ppm, grown by the HPHT method.

Sample

A blue multi-sector diamond ($\sim 7.5 \times 3.0 \times 0.5$ mm) wafer of type IIb HPHT-diamond was studied. This wafer was cut using laser cutting technology perpendicular to the $\langle 111 \rangle$ direction from the central part of a type IIb HPHT-diamond single crystal, and then mechanically polished using a polishing disk. The crystal morphology was dominated by the $\{111\}$ facets, but $\{100\}$, $\{110\}$, $\{113\}$ facets were present as well. The crystals were synthesized in a SK-850 high-pressure cubic press in a temperature range of $1450-1550°$C, at a pressure of 5.5 GPa. Boron was added to the carbon source, and a Fe-Co alloy was used as a catalyst metal with the addition of Ti and Al as nitrogen recipients. In the high-pressure cell, 4 $\{111\}$ facet oriented seeds were placed.
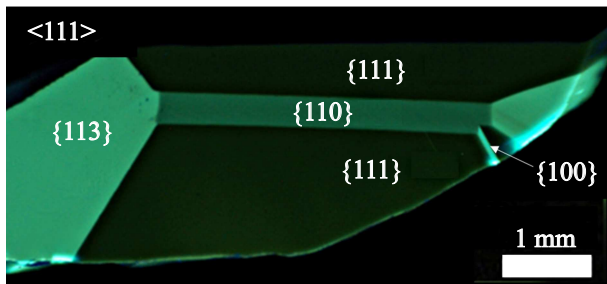
Figure 1. Photoluminescent microscopy image of the sectorial internal structure of a diamond wafer (with excitation at $\lambda = 220$ nm).

Research methods

The contents of boron impurities was assessed using IR absorption spectra. Absorption spectra were recorded on a Bruker Vertex-70 spectrometer with a Hyperion 1000 microscope in a range of $600-6000$ cm^{-1} with a resolution of 2 cm^{-1}, with averaging over 32 scans with a recording area size of $100 \times 100 \, \mu$m.

The boron concentration was determined using a known relationship [11–15]:

$$[B] \, (\text{ppm}) = 2.1 \cdot 10^{17} a_{1290} \, (\text{cm}^{-1}), \qquad (1)$$

where a_{1290} — absorption coefficient of the corresponding band.

The sectorial structure of the diamond wafer was visualized using photoluminescent microscopy using a Diamond Inspector instrument with an excitation wavelength of 220 nm. Cathodoluminescence (CL) spectra were recorded by a CAMEBAX electron probe microanalyzer (Cameca, France) equipped with an optical microscope and combined with an originally-designed cathodoluminescence station [16]. The CAMEBAX microanalyzer allows recording optical images of a sample in reflected light, measuring decay time and rise time of the luminescence at a CL-station with a time resolution of 100 ns, and recording spectra CL radiation with a spatial resolution of 1 μm. The CL spectra were recorded with an accelerating voltage of 15 keV, a current of 20 nA and an electron beam diameter of 3 μm at 77 K.

Results and discussion

The luminescent microscopy

Fig. 1 shows luminescent microscopy images of the sample. The images show a contrast typical for HPHT-diamonds. Based on the morphology of the crystal and the arrangement of growth pyramids of facets of simple shapes, (100), (111), (110) and (113).

growth sectors were identified.

Impurity composition and IR absorption spectra

Due to the high concentration of boron in the sample with a thickness of 0.5 mm, the wafer is transparent only

Table 1. Concentrations of boron in different sectors of the diamond

Sector	B, ppm (1290 cm^{-1})	B, ppm (calculation according to the diagram [18])
[111]	60 ± 6	–
[110]	–	19 ± 2
[113]	–	9 ± 2
[100]	–	1.0 ± 0.2

in the range $400-800$ cm^{-1}. To reduce the optical density, the sample on one side of the (111) sector was thinned to a wedge-shaped shape with a thickness of approximately 10 μm.. The IR absorption spectrum was recorded in a wedge-shaped part with a thickness of $30-50 \, \mu$m.

Figure 2 shows the IR absorption spectra recorded in the growth sector (111) of a diamond wafer and a wedge made from the same wafer. Large noises in the absorption spectra are explained by the low transmittance of this region. Various defects and impurities [12] can contribute to absorption in the single-phonon region of the IR spectrum of diamond crystals in the range $1100-1400$ cm^{-1}. However, in this case, with a thickness of 40 μm, the characteristic shape and peak of the 1290 cm^{-1} band, located at this thickness in the transmission region, is visible. This band in diamonds with a high boron concentration is characteristic and the main one when calculating the concentration of boron impurities.

In the works [17,18], diamonds doped with boron were studied, which were synthesized under similar conditions on the same pressing equipment as the sample studied in this article. In this work, as in more previous ones, nitrogen and other impurities were not detected in the diamonds under study; the detection limit is < 0.5 ppm. The calculation of the boron concentration in the sector (111) from the IR spectra is given in Table 1.
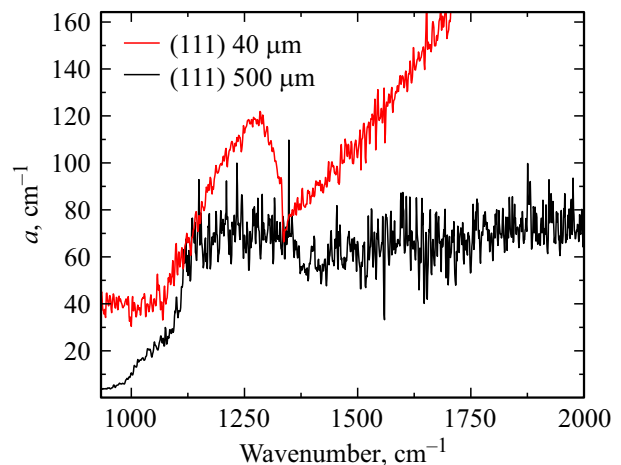
Figure 2. IR absorption spectra obtained for different sample thicknesses in the region of the (111) growth sector of type IIb HPHT diamond.
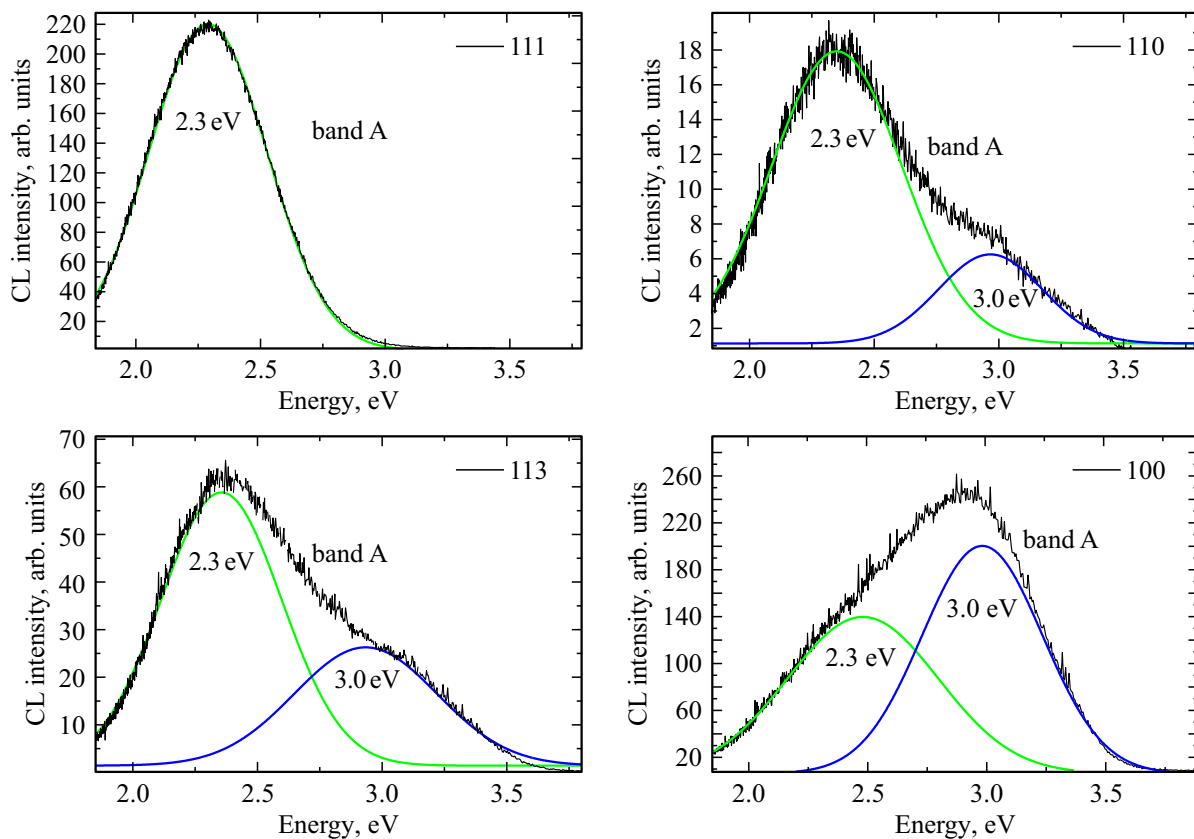
Figure 3. CL spectra of the sample at 77 K, obtained for different growth sectors of the sample under study.

Also in the work [18] a diagram of the distribution of boron impurities by sectors is demonstrated, which allows to evaluate the boron content in all sectors if the reliable boron content in at least one of the sectors is known. Calculation of boron concentration according to the diagram [18] is given in Table 1.

CL studies

The CL spectra of the identified growth sectors of the diamond wafer are presented in Fig. 3. The shape of the CL spectra for each sector corresponds to a superposition of the broad bands of 2.3 and 3 eV observed in diamonds. The most intense luminescence of the 2.3 eV band is observed in the $\langle 111 \rangle$ sector. The intensity of the band does not depend directly on the boron content, but probably correlates with the nitrogen content. In the work [19] the ratio of nitrogen in diamond was determined as $1:10:46:100$ for sectors, respectively $(110):(113):(100):(111)$. From Fig. 3 a direct correlation is visible between the intensity of the CL band 2.3 keV and the ability of the face to capture nitrogen impurities. The relative intensity of the band with a maximum of 3.0 eV increases with decreasing boron concentration.

The luminescence decay times of the bands with maxima of 2.3 and 3.0 eV are presented in Table 2 and correlate with the literature data of the band A time analysis A [20]. And there is no direct correlation between luminescence decay times and boron concentration.

Table 2. Temporal characteristics of the studied luminescence bands

Sectoe	Band luminescence decay time		
	2.3 eV		3.0 eV
	$t_1, \mu s$	$t_2, \mu s$	t_1, ns
(111)	96 ± 4	11 ± 1	< 100
(110)	19 ± 3	2 ± 1	< 100
(113)	90 ± 3	10 ± 1	< 100
(100)	71 ± 3	5 ± 1	< 100

It can be seen from the data obtained that each sector is a separate luminescent material with its own characteristic luminescent properties. The recombination model of luminescence assumes [6,20] the existence of a dependence of the position of luminescence band maximum on the concentration of the donor and acceptor

$$E(r) = E_g - (E_{ac} - E_d) + e^2/\varepsilon r,$$

where $E(r)$ is photon energy, $E_{+}g$, E_{ac}, E_d is band gap and position of the acceptor and donor levels, respectively, e is electron charge , ε is dielectric permittivity, r is distance between donor and acceptor. At this stage of research, no shift in the maximum of the 2.3 and 3.0 eV bands in sectors with different boron concentrations was noticed [18].

Apparently, each sector has various ratio of boron and nitrogen, and, accordingly, its own set of defects in the crystal structure and the ratio of donor-acceptor pairs. To determine the nature of the 2.3 and 3.0 eV bands, it is necessary to study the luminescence characteristics in samples with reliably controlled concentrations of both boron and nitrogen, or find a way to independently determine the nitrogen concentration for growth sectors saturated with boron.

Conclusions

This work shows that the luminescent properties of the growth sectors of HPHT diamond weakly correlate with the boron content. Each growth facet is a separate luminescent material with its own characteristic CL properties. Thus, it is required to compare the properties of certain growth sectors of various diamonds.

Funding

Conflict of interest

The authors declare that they have no conflict of interest.

References

[1] G.T. Williams, J.A. Calvo, F. Dodson, T. Obeloer, D.J. Twitchen. *17th IEEE Intersociety Conference on Thermal and Thermomechanical Phenomena in Electronic Systems* (ITherm), San Diego, USA, 235–239 (2018).

[2] T. Shao, F. Lyu, X. Guo, J. Zhang, H. Zhang, X. Hu, A.H. Shen. Carbon., **167**, 888 (2020).

[3] A.T. Collins, E.C. Lightowlers, J.E. Field. *The properties of diamond* (Academic Press, London, UK, 1979).

[4] A.T. Collins. Semicond. Sci. Technol., **4** (8), 605 (1989).

[5] J. Walker. Rep. Prog. Phys., **42** (10), 1605 (1979).

[6] P.J. Dean. Phys. Rev., **139** (2A), 588 (1965).

[7] H. Kawarada, Y. Yokota, Y. Mori, K. Nishimura, A. Hiraki. J. Appl. Phys., **67** (2), 983 (1990).

[8] I. Kiflawi, A.R. Lang. Phil. Mag., **30** (1), 219 (1974).

[9] S.J. Pennycook, L.M. Brown, A.J. Craven. Phil. Mag. A, **41** (4), 589 (1980).

[10] N. Yamamoto, J.C.H. Spence, D. Fathy. Phil. Mag. B, **49** (6), 609 (1984).

[11] A.T. Collins, A.W.S. Williams. J. Phys. C, **4**, 1789 (1971).

[12] B. Dishler. *Handbook of Spectral Lines in Diamond* (Springer, 2012).

[13] D. Fisher, S.J. Sibley, C.J. Kelly. J. Phys.: Condens. Matter, **21** (36), 364213 (2009).

[14] S. Karna, D.V. Martyshkin, Y.K. Vohra, S.T. Weir. MRS Proc., **1519** (1), 327 (2013). https://link.springer.com/article/10.1557/opl.2012.1759

[15] G. Davies, P.L. Walker, P.A. Thrower. In: *Chemistry and Physics of Carbon, eds P.L. Walker Jr, P.A. Thrower* (Dekker, N.Y., 1977), p. 34.

[16] M.V. Zamoryanskaya, S.G. Konnikov, A.N. Zamoryanskii. Instrum. Exp. Tech., **47** (4), 477 (2004).

[17] I.V. Klepikov, A.V. Koliadin, E.A. Vasilev. IOP Conference ser., **286** (1), 012035 (2017).

[18] V.A. Kravets, I.B. Klepikov, E.A. Vasiliev. FTT, **11**, 1995 (2023) (in press).

[19] R. Burns, V. Cvetkovic, C.N. Dodge, D.J.F. Evans, M.-L.T. Rooney, P. Spear, C. Welbourn. J. Crystal Growth, **104** (2), 257 (1990).

[20] P.B. Klein, M.D. Crossfield, J.A. Freitas Jr, A.T. Collins. Phys. Rev. B, **51** (15), 9634 (1995).

Translated by 123